



# NIRSpec Performance Report

## NPR-2012-002

Authors: Guido De Marchi  
Date of Issue: 1 September 2012  
Version: 1

## Calibration of the GWA position sensors – Part I

### Abstract:

We have calibrated the position/tilt sensors of the NIRSpec grating wheel assembly (GWA) using the data collected during the first NIRSpec flight model ground calibration campaign. In this report we investigate the effects of the GWA repositioning uncertainty on the accuracy of the target acquisition process and of the wavelength calibration, showing that using the sensors' readings the required accuracy is met with ample margin.

### 1 INTRODUCTION

The NIRSpec Grating Wheel Assembly (GWA) contains eight selectable optical elements, providing dispersion into spectra as well as imaging of the FOV for target acquisition. Any rotational non-repeatability of the GWA will result in a small shift of the image or spectrum at the detector plane. Therefore, for good science performance these shifts have to be minimised, accurately known and corrected for if too large.

In order to guarantee high mechanical angular reproducibility, a ratchet is used to achieve accurate positioning of the selected GWA optical element. This ratchet comprises two flexural pivots, pointing in the same direction as the wheel axis, which is parallel to the optical bench. The ratchet subassembly is mounted on the mechanical support structure of the GWA. A spring draws the top part of the ratchet onto the index bearings, which reside on the wheel structure. The wheel can reside in eight different equilibrium positions, corresponding to the seven dispersive elements and the mirror.

The mechanical angular reproducibility of the GWA mechanism is very good due to the very high quality bearings and ratchet assembly. Typically the reproducibility is  $\sim 2.5$  arcsec ( $1 \sigma$ ). However, for optimal scientific performance this is not sufficient, as this small angular variation already changes the position of the image on the detector plane by  $\sim 0.4$  pixel. This mechanical angular reproducibility is too large to accept for two main reasons:

1. Spectral calibration. Due to the non-perfect GWA reproducibility, after each repositioning, the NIRSpec spectra from the same slit will not fall exactly in the same place on the detector, but will be shifted along the dispersion direction. The required accuracy for wavelength calibration is  $1/4$  of a pixel or  $1/8$  of a spectral resolution element. Thus, the GWA should place a spectral feature of known wavelength always at the same detector position along the dispersion direction, to within  $1/4$  of a pixel, but the repositioning uncertainty can cause shifts of one pixel or more.

2. Target acquisition. The objects to be studied must be accurately placed at the centre of the corresponding apertures (fixed slits, MSA or IFU), located at the instrument's intermediate focal plane (i.e. the MSA plane). This is achieved using reference stars in the same field, whose pixel positions can be accurately determined on the detector. However, the coordinate transformations between the plane of the detector and that of the slits crucially depend on the positional accuracy of the GWA. A maximum allowable contribution of 5 mas on the sky (or  $\sim 1/20$  of a pixel) has been allocated for these uncertainties in the target acquisition error budget. This translates into a required angular knowledge of the actual GWA optical element orientation of  $\sim 0.3$  arcsec, or about 10 times better than the typical mechanical angular reproducibility of the GWA.

To overcome these limitations, a grating wheel tilt sensor system has been developed and installed on NIRSpec in order to provide a much better knowledge of the actual orientation of the selected GWA optical element (see Weidlich et al. 2008 and Leikert 2011). In this report we use measurements collected during the first NIRSpec ground-based cryogenic calibration campaign (hereafter Cycle 1; see Ferruit et al. 2011 and Birkmann et al. 2011) to show that the magneto-resistive position sensors installed on the wheel provide very accurate information on the position of the wheel itself, thereby enabling an efficient acquisition of the science targets and proper wavelength calibration.

## **2 DESCRIPTION OF THE TILT SENSORS**

Two tilt sensors are mounted on the GWA, one to measure the actual orientation of the GWA optical elements along the dispersion direction and the other along the cross-dispersion direction. The accuracy of the orientation along the dispersion direction is most critical for NIRSpec's performances and we address it in this paper. The performances in the cross dispersion direction are the topic of a forthcoming report (Part II).

A magnet pair is mounted onto the grating wheel structure for each of the eight optical elements. Each pair of magnets provides a slit for transit over the sensor field-plates, which are fixed to the support structure and electrically setup in a bridge configuration. Inside the slit, the magnetic field is strong and well collimated and the displacement of the magnets is detected by the field-plates. The latter (of type Infineon FP 420L90B) are fully functional in the temperature range between 4 K and 300 K.

As an example, the left panel of Figure 1 shows the four field plates of the nominal sensor unit (marked 1 through 4) at a single location. The angular deviations are derived from

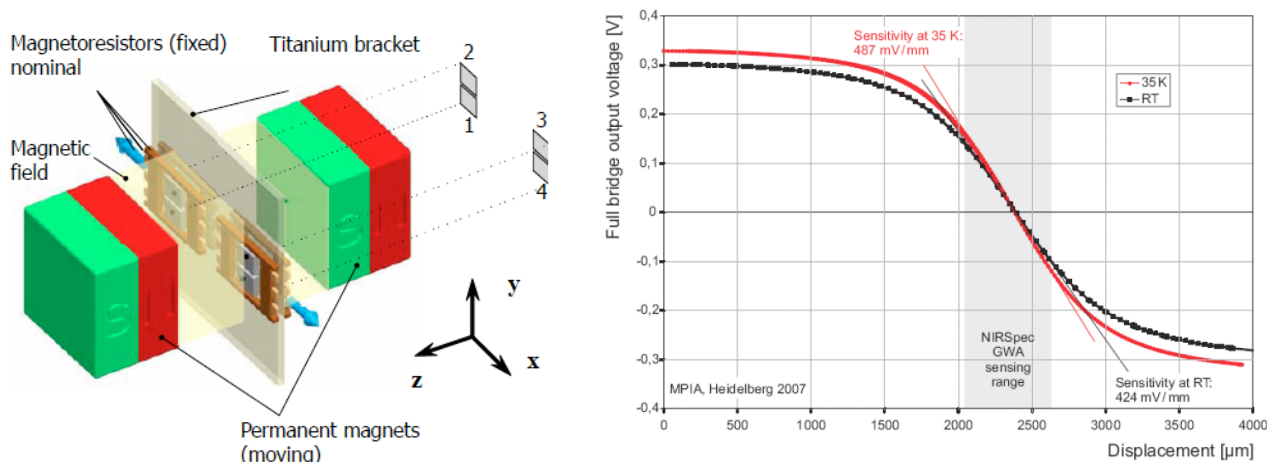


Figure 1. *Left*: Schematic view of the 1-D magneto-resistive position sensor. Four field plates (1–4) on the same side of the holder are located in the strong magnetic field region between a sensor magnet pair providing the nominal signal. *Right*: Test results for the sensitivity of the GWA position sensor based on four magnetic field plates in full bridge configuration for a supply voltage of 0.5 V. The two curves refer to the sensitivity at 35 K and at room temperature (RT).

lateral displacements along the direction indicated by the arrows. The position sensitivity, as shown in the right panel, depends on the steepness of the spatial gradient of the magnetic field strength along the direction indicated in Figure 1. A sensitivity of approximately  $400 \mu\text{V} \mu\text{m}^{-1}$  in the most sensitive range of the sensor bridge relates to 0.2 arcsec angular resolution of the wheel based on a sensitivity of  $20 \mu\text{V}$  of the readout electronics.

The readout voltage of the sensor bridge is acquired by the instrument flight software at the end of every GWA reconfiguration and is stored in the telemetry stream. Different operational schemes are possible for acquiring the voltage and they provide readings with different accuracies. The most accurate results are obtained when the voltage is sampled 256 times and the values obtained in this way are corrected for any offsets in the sensor supply voltage and averaged together. The drawback is that this procedure takes of order 30 s, thereby potentially reducing the overall efficiency of science operations. Since there are circumstances in which an approximate knowledge of the voltage reading is sufficient, it is also possible for the flight software to request just one instantaneous reading of the sensor bridge voltage, without corrections for the sensor supply voltage. Both types of operational schemes have been used during Cycle 1 and the corresponding results are discussed in Section 4.

Finally, an alternative approach is possible in which the number of times that the voltage is polled is a configurable parameter between 1 and 100 (referred to as REC mode). The values provided in the telemetry correspond to the readout voltage of the sensor bridge and are corrected for the supplied offset and gain, although the sensor supply voltage is not included in the calculation. The advantage of this approach is the reduced overhead, since for a typical value of 25 reads the command execution time is reduced to about 6 s. The suitability of this mode of operations will be tested during Cycle 2.

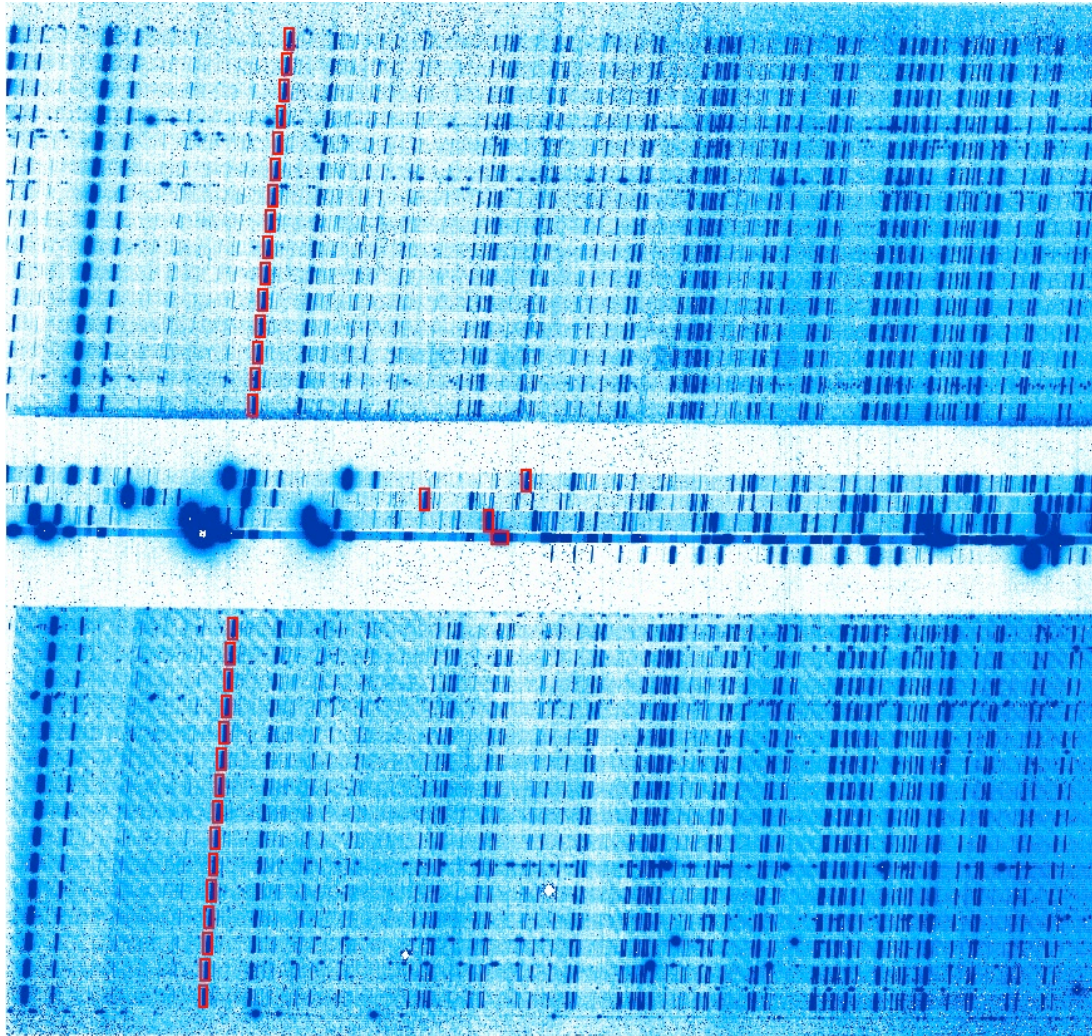


Figure 2. Count-rate image showing the ARGON spectral source as observed in IFU mode, through the G140H grating. The rectangular apertures correspond to regions including (unresolved) spectral features that were used to determine the absolute positions of the spectra. Only one detector is shown here.

### 3 MEASUREMENTS

In the course of Cycle 1, we collected a large number of spectra in various configurations through all eight optical elements installed in the GWA. For each optical element, the same illumination source was used more than once throughout the campaign to obtain spectra. Since these spectra were obtained with the same source through the same GWA element, they should fall exactly at the same location on the detector, except for any shifts introduced by the mechanical inaccuracies of the GWA mechanisms. Provided that there are enough measurements with the same GWA and source combination, and that one or more GWA movements have been commanded between these exposures, we can use these data to study the mechanical accuracy of the GWA and the performances of the tilt sensor.

Particularly useful are the exposures that contain clearly identifiable (possibly unresolved) spectral features, which more easily allow us to determine the position of the spectra on the



Figure 3. Count-rate image showing the ULS source observed in IFU mode, through the PRISM. The laser emission line source is clearly visible. Only a portion of the frame is shown, containing the fixed slits and some of the IFU virtual slits. The spectra from some failed open MSA shutters are also visible.

detector plane along the dispersion direction. These observations include spectra obtained with the external Argon emission line source (hereafter ARGON), with the external unresolved line source (a laser source; hereafter ULS), and with the external and internal rare earth (Erbium) absorption line sources (hereafter SR1 and REF, respectively).

Examples of these observations are provided in Figures 2, 3 and 4. Figure 2 shows the ARGON source observed with NIRSPEC in IFU mode, through the G140H grating (note that only one of the two detectors is shown here, covering approximately the wavelength range between 1.0 and 1.4  $\mu\text{m}$ ). Figure 3 shows the ULS source with the PRISM in IFU mode, although only a part of the image is shown, containing the fixed slits and some of the IFU virtual slits (note that also some failed open shutters provide spectra). Figure 4 shows the SR1 source in IFU mode, through the G140M grating combined with the F140X filter, which limits the wavelengths to the range from 1.3 to 1.7  $\mu\text{m}$  (note that the spectra corresponding to the fixed slits and to some of the IFU virtual slits are shown magnified on the right-hand side of the figure, on top of the second detector, in regions normally not occupied by other spectra).

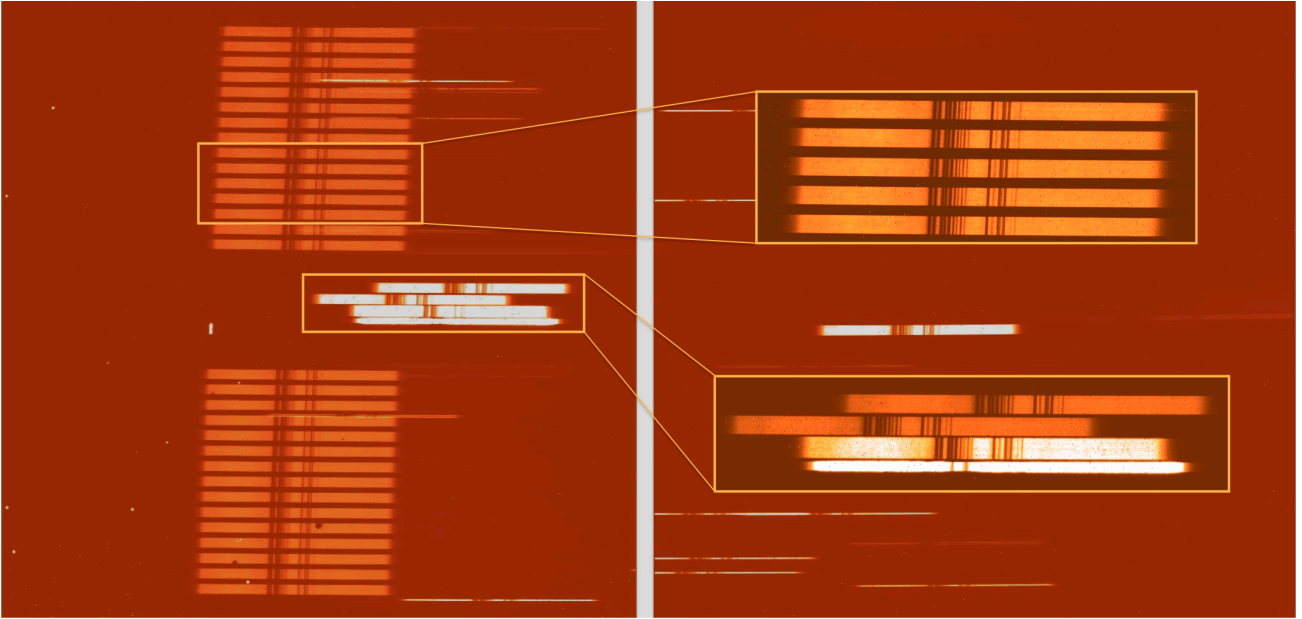


Figure 4. Count-rate image showing the SR1 source in IFU mode, through the G140M grating and F140X filter. The filter only transmits wavelengths in the range from 1.3 to 1.7  $\mu\text{m}$ . The insets show a magnified version of the spectra corresponding to the fixed slits and to some of the IFU virtual slits.

All exposures considered in our analysis are count-rate maps generated by the NIRSpec pre-processing pipeline (Birkmann 2011), which takes care of dark and bias subtraction, hot pixel masking, flat fielding and linearity correction. These steps are necessary in order to prevent biases in the determination of the actual pixel position of the spectral features.

## 4 DATA ANALYSIS

We have developed an IDL procedure that takes as input observations of the type shown in Section 3 and determines the pixel position of a number of predefined unresolved spectral features, such as those marked by the boxes shown in Figure 2. Details on how to invoke the IDL procedure are given in the Appendix, while the main steps are briefly summarised here.

The procedure takes as input a list of exposures corresponding to observations taken at different times but through the same spectral/source configuration and extracts from each of them a predefined number of regions where the spectral features are expected to be located. The extracted regions have the same exact pixel coordinates in all exposures, but since the GWA has moved between these reconfigurations, the spectral features themselves will be at (slightly) different pixel positions. A simple cross-correlation routine is used to determine the displacement of the spectral features between exposures and since many regions are considered in each exposure also a reliable uncertainty can be derived. By correlating the displacements derived in this way with the readings of the GWA magneto-resistive tilt sensors, stored in the telemetry of each exposure, one can calibrate the sensors and verify their performances. Examples of the excellent correlations between pixel shifts and the corresponding voltages of the sensor bridge are shown in Figures 5, 6 and 7.

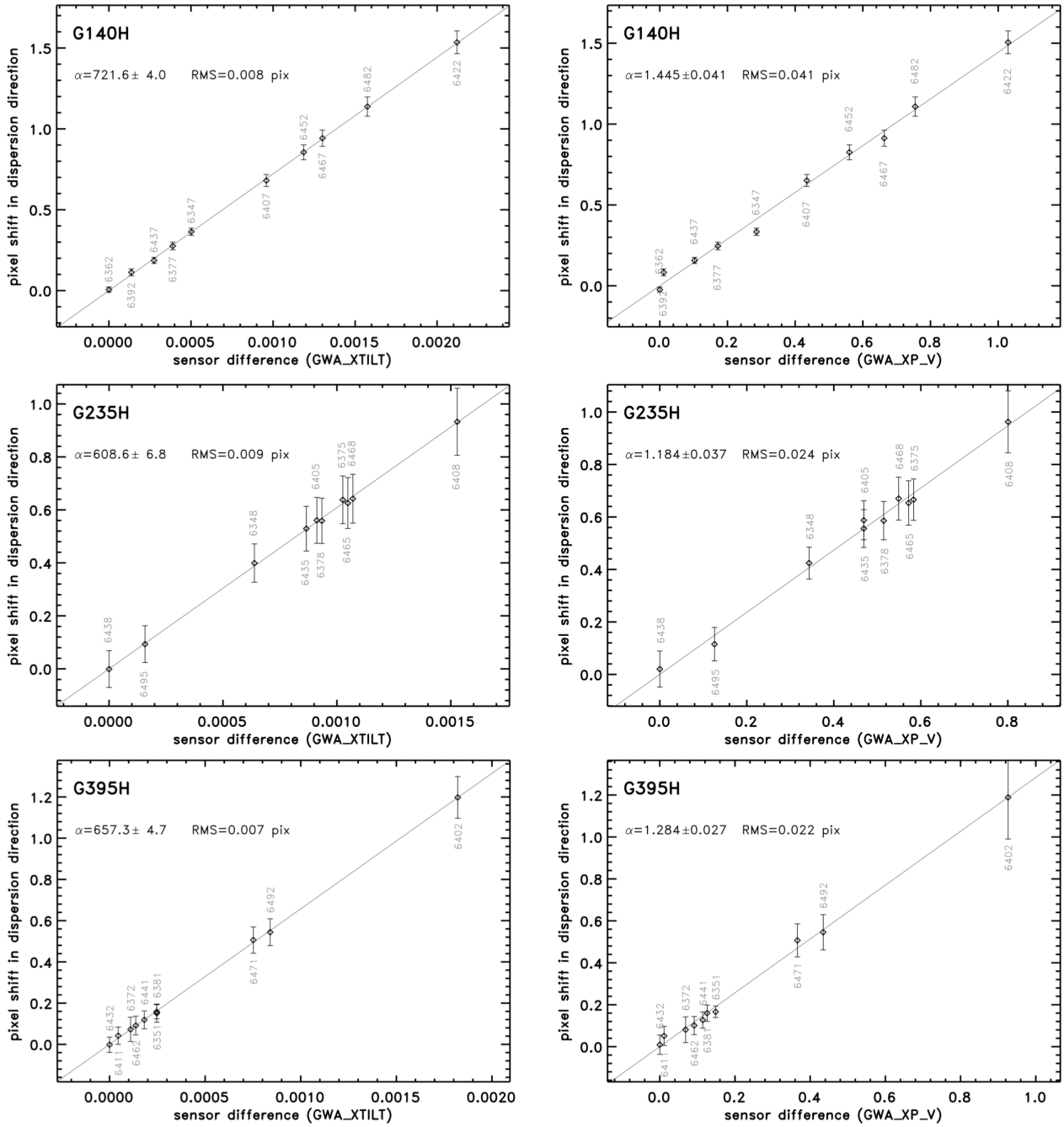


Figure 5. Relative pixel shift measured along the dispersion direction as a function of the readings of the GWA tilt sensor for the three NIRSPEC high-resolution gratings. The panels on the left refer to the averaged readings stored in the GWA\_XTILT keyword, whereas those on the right show the instantaneous readings stored in keyword GWA\_XP\_V. In both cases a linear fit (solid lines) reproduces the observations rather well. The slope ( $\alpha$ ) and residuals (RMS) of the fits are also given. Each observation is identified by the corresponding entry number in the exposures database.

In Figure 5 we show the results for the three high-resolution gratings G140H, G235H and G395H, combined with the ULS source. In all panels, the observed pixel shift is plotted as a function of the difference in the voltage reading, taking as a reference the observation with the smallest voltage value in each series (observations are identified by the labels next to

the data points, each label showing the corresponding entry numbers in the exposures database; see Giardino & Sirianni 2011 for details on the structure of the database). The panels on the left-hand side have been obtained using the most accurate value of the reading, which as we mentioned in Section 2 is obtained by polling the voltage of the sensor bridge 256 times and taking the average, after having corrected the individual values for any offsets in the sensor supply voltage. The corresponding header keyword is GWA\_XTILT. For the panels on the right-hand side we have used instead the instantaneous reading of the sensor bridge voltage, stored in the header keyword GWA\_XP\_V. Each point in these graphs corresponds to a separate exposure and the error bars reflect the scatter in the displacement of different features in the same exposure (e.g. the different boxes in Figure 2). In some cases, the error bars are smaller than the size of the symbols (note that an error bar is also shown for the reference exposure since it reflects the small uncertainties inherent in the Lorentzian fit to the cross-correlation profile).

First and foremost, it is evident that the uncertainties in the mechanical angular reproducibility of the GWA result in offsets of up to  $\sim 1$  pixel in the detector plane, as mentioned in the Introduction. However, it is also clear that in all cases the pixel offsets correlate very well with the sensor readings. Regardless of the specific voltage reading utilised, a linear dependence of the type  $\Delta X = \alpha \Delta V$  (see solid lines) offers an excellent fit to the observations, where  $\Delta X$  is the pixel offset and  $\Delta V$  the difference in the voltage readings. The values of the slopes  $\alpha$  and of their uncertainties are provided in each panel. As expected, each grating has a different value of  $\alpha$ , due to the intrinsic differences in the way the magnet pairs are mounted onto the grating wheel structure for each of the eight optical elements.

To better characterise the differences between the two types of reading (averaged vs. instantaneous), we show in Figure 6 an example for the case of the G140M grating. The diamonds and crosses correspond, respectively, to the averaged and instantaneous voltages (the ordinates being the same, since the pixel shift is measured on the same exposure). The abscissae for the crosses have been obtained by translating the values of GWA\_XP\_V to GWA\_XTILT using the linear best fits, for illustration purposes. Taking as a reference the relationship based on the GWA\_XTILT readings (solid line), the pixel offsets implied by the GWA\_XP\_V readings could deviate by as much as  $\sim 0.05$  pixel, which is uncomfortably close to the maximum uncertainty allowed by the target acquisition requirements. As we will conclude in Section 5, the average values of the sensor bridge voltage are to be preferred to the instantaneous readings when correcting for the uncertainties caused by the GWA mechanical reproducibility.

Besides depending on the specific GWA optical element, the relationship between voltage reading and pixel offset is a function of the temperature of the optical bench, as we show in Figure 7. In order to test the instrument's performances at the extremes of the planned range for operations, in the course of Cycle 1 NIRSpec underwent a planned reset of the temperature of the optical bench, from 31 K to 45 K. The two sets of data points in each panel correspond to two different temperatures, namely 31 K for the upper series and 45 K for the lower one. As an example, the figure shows the case of the imaging mirror and of the prism. As before, the set of panels on the left-hand side correspond to the GWA\_XTILT telemetry keyword, whereas those on the right-hand side are for the less accurate

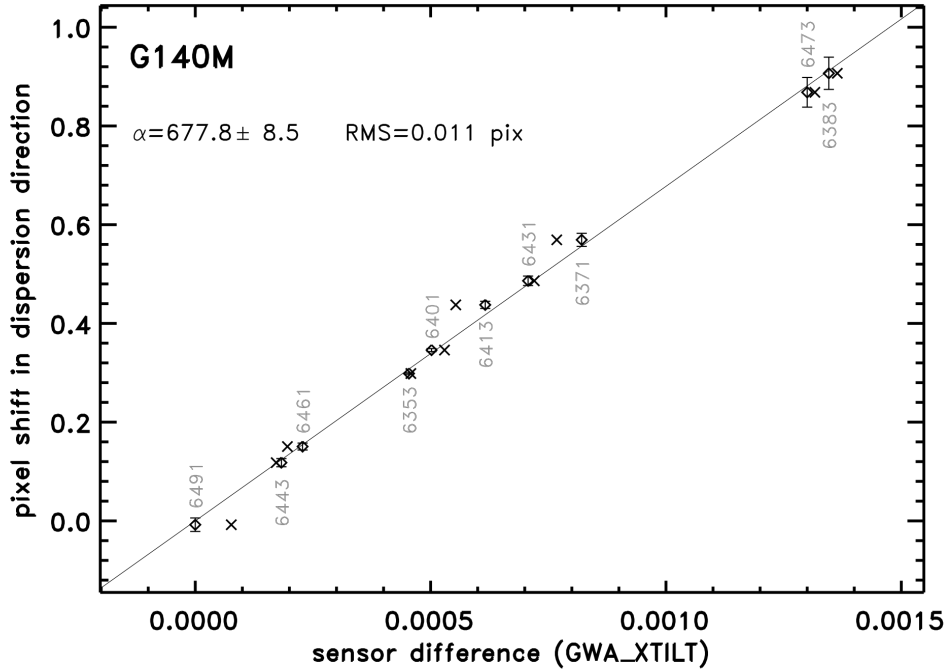


Figure 6. The measured pixel shifts for the G140M grating are shown as a function of the average voltage readings (diamonds) and instantaneous readings (crosses). The latter are noisier and hence less accurate.

GWA\_XP\_V instantaneous reading. The relationship between measured pixel offset and sensor reading remains remarkably linear over the entire temperature range for NIRSpec operations, thereby confirming the expected performances of the sensors (see Section 2). It is however clear that the slopes of the relationships are different, as indicated by the values of  $\alpha$  shown in each panel (the same is true for all other GWA elements). This means that the actual relationship between sensor readings and pixel offsets to be used for in flight operations will have to be determined once again, for the specific operating temperature achieved in orbit.

## 5 DISCUSSION AND CONCLUSIONS

The analysis presented in Section 4 confirms that the magneto-resistive position sensors installed on NIRSpec's GWA provide very accurate information on the position of the wheel itself. While the mechanical reproducibility of the wheel leaves uncertainties of  $\sim 0.5$  pixel on the position of spectral features on the detector, the value of the sensor bridge voltage provides a much higher accuracy on the actual position of the wheel. In particular, our analysis of a large number of observations shows that the relationship between pixel offset in the dispersion direction and sensor bridge voltage reading is remarkably linear, with very small residuals. The root mean square deviations from the linear fits are typically 0.009 pixel for the gratings, 0.018 pixel for the prism and 0.029 pixel for the mirror. Note that these values are in all cases upper limits to the actual uncertainties, particularly for the prism and the mirror, caused by the limitations in our measurement accuracy. Nevertheless, these uncertainties are comfortably smaller than those required for efficient

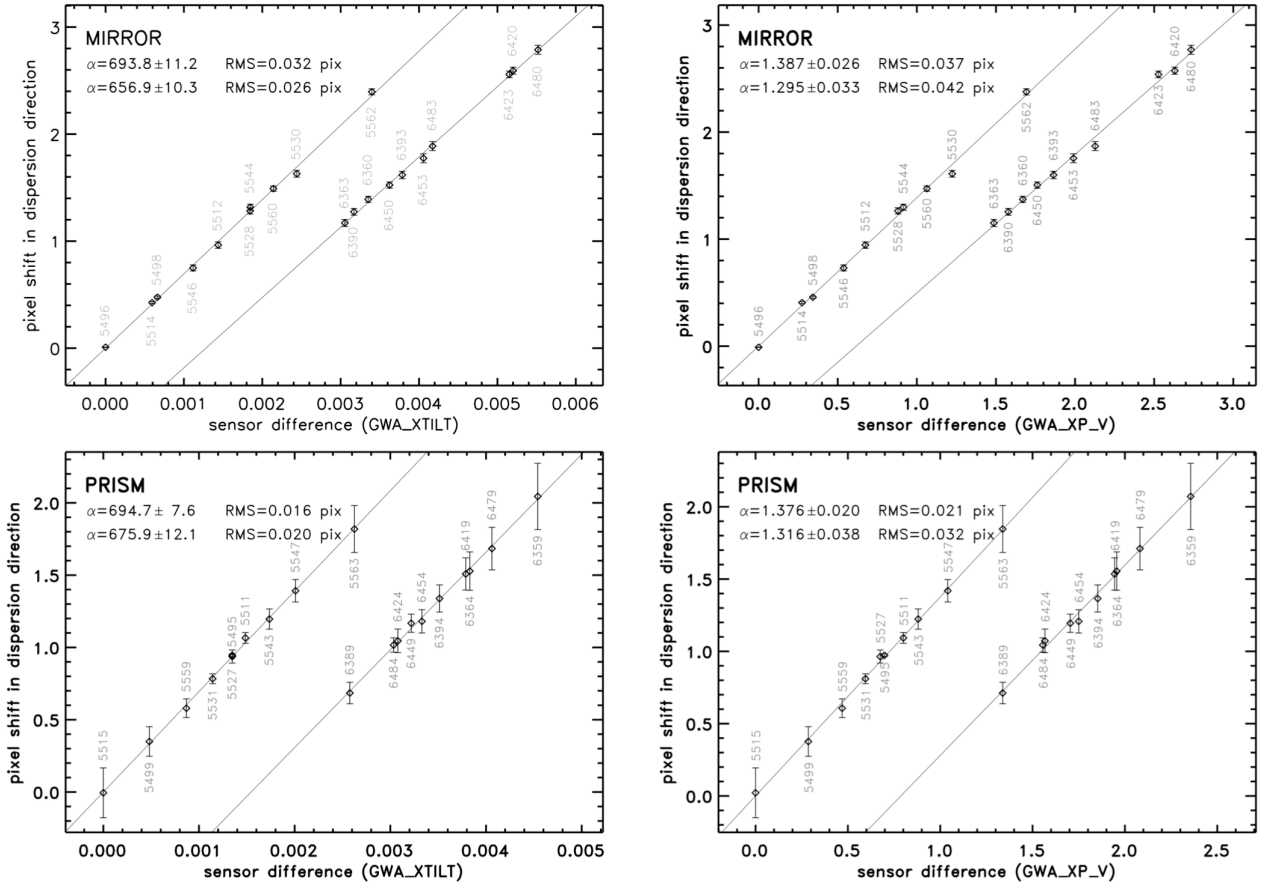


Figure 7. Same as Figure 5 but for a different set of optical elements (MIRROR and PRISM). The two sets of data-points in each panel correspond to two different temperatures of the optical bench, 31 K (upper) and 45 K (lower). The observed distributions are remarkably linear.

NIRSpec operations. More precisely, the zero point in the wavelength calibration requires an accuracy of better than 0.25 pixel and even in the “worst” case (PRISM) the accuracy that we achieve is more than an order of magnitude better. For the more demanding target acquisition procedure, the maximum allowable contribution to the overall error due to the GWA repositioning uncertainty is 5 mas on the sky, corresponding to  $\sim 0.05$  pixel, and the accuracy that we achieve is about a factor of two better in stable temperature conditions.

This implies that it will be possible to accurately determine the pixel offset caused by the repositioning uncertainties of the GWA from the value of the sensor bridge voltage, obtained and stored in the telemetry after each GWA reconfiguration. In practice, offsets with respect to a reference value of the sensor reading will be calculated by the calibration pipeline (for wavelength calibration) and by the flight software (for target acquisition) using a pair of coefficients (intercept and slope) for each GWA element, derived with the procedure presented in this paper.

In practice, for each grating wheel element there will be a reference value of the two GWA voltage keywords, i.e. a reference voltage value  $V_{x,0}$  for the dispersion direction and  $V_{y,0}$  for the cross-dispersion direction, corresponding to the nominal position of images and

spectra on the detectors. There will also be a pair of coefficients ( $\alpha$  and  $\beta$ ) relating voltage differences to pixel offsets (see Figures 5, 6 and 7) in the dispersion and cross-dispersion directions. As regards the target acquisition procedure, the on-board script will read the GWA telemetry keywords, i.e. the  $V_{x,m}$   $V_{y,m}$  values of the measured voltages of the sensors in the dispersion and cross-dispersion directions, and will correct the centroids ( $X_m$ ,  $Y_m$ ) of the reference stars to bring them to their nominal ( $X_o$ ,  $Y_o$ ) coordinates according to the following equations:

$$X_o = X_m + \alpha (V_{x,o} - V_{x,m}) \quad (1)$$

$$Y_o = Y_m + \beta (V_{y,o} - V_{y,m}) \quad (2)$$

Our work, however, has also shown that the actual coefficients depend on two additional parameters, namely the specific type of sensor reading used and the temperature of the optical bench, both of which will determine the actual coefficient values for in-orbit operations.

As regards the type of sensor reading, our work shows that, when the voltage is polled 256 times and the values obtained in this way are corrected for the offsets in the sensor supply voltage and averaged together to reduce the noise (telemetry keyword GWA\_XTILT), the residuals are typically twice as small as when the value of the voltage is read out only once, without any further corrections (telemetry keyword GWA\_VP\_X). Since the first mode of operation requires a considerably longer time to execute (of order 30 s), we plan to test an alternative approach during the second NIRSpec cryogenic campaign, scheduled for late 2012, during which a different operational scheme will be followed to read a limited number of times the voltage of the sensor bridge and to correct it for any offsets and gain differences. The advantage of this approach is the reduced overhead, since for a typical group of 25 reads the command execution time is only about 6 s longer than that for instantaneous reading. If the accuracy reached with this mode of operation is shown to meet our stringent requirements for wavelength calibration and target acquisition, it will allow potentially significant efficiency improvements.

As for the temperature dependence of the performances of the GWA tilt sensors, it is clear that the actual relationship between pixel offsets and tilt sensor readings to be used in orbit will have to be determined once again after launch, for the specific range of operational temperatures applicable at that time. This can be efficiently achieved using the internal Erbium absorption line source (REF source), which can be effectively coupled with all high- and medium-resolution dispersive elements, without requiring any external observations of astronomical sources (for the PRISM, the special LINE4 source will be used). Extended tests with the internal Erbium source are already planned for Cycle 2. Furthermore, the forthcoming calibration campaign will allow us to test even more extensively the long-term stability of the sensors and to look for possible drifts, since Cycle 2 will cover a longer time span than Cycle 1 and will make a more intensive use of the internal mechanisms.

In conclusion, the analysis presented here demonstrates that, thanks to the sensors installed on the GWA, it is possible to predict the shift between reconfigurations of any spectral feature of known wavelength with an accuracy higher than that required for wavelength calibration and for target acquisition. At the moment, the baseline approach for the NIRSpec target acquisition process foresees the use of short exposures with the internal

continuum lamp, in order to derive the exact tilt of the GWA imaging mirror from the location of the fixed slit images on the detector. Although this approach remains for now unchanged, if the levels of accuracy derived so far are consistently reached during Cycle 2 and throughout the commissioning and early operations phase, as we expect, it should be possible to reduce the need for internal calibration exposures, thus saving both time and usage of NIRSpec's internal mechanisms.

## 6 REFERENCES

- Birkmann, S. 2011, "Description of the NIRSpec pre-processing pipeline," NTN-2011-004 (Noordwijk: ESTEC)
- Birkmann, S. M., Ferruit, P., Böker, T., De Marchi, G., Giardino, G., Sirianni, M., Stuhlinger, M., Jensen, P., te Plate, M., Rumler, P., Dorner, B., Gnata, X., Wettemann, T. 2012, "The Near Infrared Spectrograph (NIRSpec) on-ground calibration campaign," Proc. SPIE 8442-123
- Ferruit, P. 2011, "Overview of the NIRSpec first cryogenic test campaign", NTN-2011-001 (Noordwijk: ESTEC)
- Giardino, G., Sirianni, M. 2011, "NIRSpec Archive and Database," NTN-2011-003 (Noordwijk: ESTEC)
- Leikert, T. 2011, "Alignment and testing of the NIRSpec filter and grating wheel assembly," Proc. SPIE 8131-25
- Weidlich, K., Fischer, M., Ellenrieder, M.M., Gross, T., Salvignol, J.C., Barho, R., Neugebauer, C., Königsreiter, G., Trunz, M., Müller, F., Krause, O. 2008, "High-precision cryogenic wheel mechanisms for the JWST NIRSpec instrument", Proc. SPIE 7018, 64

## APPENDIX

The IDL procedure developed for this analysis is contained in the file `gwa_sens.pro`, located in the subdirectory `/Software/JWST_IDL/lib/nirspec/misc/` of the CVS repository. The syntax for invoking the procedure is as follows:

```
IDL> gwa_sens, 'selection_string', output [, flags]
```

The string `selection_string`, to be surrounded by quotation marks, contains the search criteria for the exposures to be analysed. It is automatically generated and printed on the screen every time the `nar_find` procedure is used to query the exposures database. The most practical way to feed the string to the procedure is to copy and paste it with the mouse. Since a change of bench temperature occurred during Cycle 1, the procedure treats separately exposures taken before and after the change (corresponding to NID=6263), providing two series of results, i.e. fitting coefficients and related uncertainties. A third series of coefficients will be added for exposures to be taken in Cycle 2.

The parameter `output` is the name of a IDL structure-type variable that will contain the results of the fit. There are currently two series of results in the structure, for the two temperature ranges, and a third one will be added in preparation for Cycle 2. Each series contains the following elements:

<code>NID[1 2 3]</code>	entry number in the exposures database; one per exposure
<code>XTILT[1 2 3]</code>	value of the sensor telemetry, either <code>GWA_XTILT</code> or <code>GWA_XP_V</code> depending on the <code>/VOLT</code> optional flag (see below); one per exposure
<code>AVGSH[1 2 3]</code>	average value of the shifts in dispersion direction for the exposure with respect to the reference exposure; one per exposure
<code>SIGSH[1 2 3]</code>	uncertainty (standard deviation) of the shifts; one per exposure
<code>Q[1 2 3]</code>	value of the intercept of the best linear fit to the distribution
<code>SIGQ[1 2 3]</code>	uncertainty (standard deviation) on <code>Q</code>
<code>M[1 2 3]</code>	value of the slope of the best linear fit to the distribution
<code>SIGM[1 2 3]</code>	uncertainty (standard deviation) on <code>M</code>
<code>RMS[1 2 3]</code>	root mean square dispersion around the best linear fit

The optional `flags` are as follows:

`/FS` to only consider apertures corresponding to the fixed slits

`/VOLT` to use the bridge voltage values stored in `GWA_XP_V` rather than in `GWA_XTILT`

The procedure reads in the exposures identified by `selection_string` and determines the observing mode and illumination source in use. Only the first exposure in the list is checked and is used as a reference, so it is important that all exposures be of the same type (note that currently the procedure does not process subarrays). Once the configuration is determined, the procedure loads the corresponding `ds9` region file containing the locations of the “apertures”, i.e. rectangular regions of the detectors at predefined pixel positions around which spectral features are expected. The region files are searched in the local working directory and if not found an error message is generated on the screen. Region files can be modified as needed, provided that the first four regions refer to the fixed slits and any other region is used for the IFU. The regions must be rectangles.

Using the region files, the procedure extracts from each exposure the corresponding regions and, through cross-correlation, determines the shift between these regions and the corresponding regions in the first frame, taken as a reference. Once all images are processed, the best linear fit is searched to determine the relationship between pixel shifts and corresponding voltage readings. The results are shown graphically on the screen, printed in a postscript file (whose name is shown on the screen) and the best fitting parameters are stored in an ASCII file with the same name (extension `.txt`) and saved in the named structure (`output`). Files are overwritten every time, so it is necessary to rename them if they are to be saved.